Received: 10 May 2021 | Revised: 17 July 2021 | Accepted: 12 August 2021

DOI: 10.1002/leg3.121

ORIGINAL ARTICLE

Legume Science Open Access WILEY

The effects of crosslinking agents on faba bean flour–chitosan-curcumin films and their characterization

Eda Yildiz | Esmanur Ilhan | Leyla Nesrin Kahyaoglu | Gulum Sumnu | Mecit Halil Oztop

Department of Food Engineering, Middle East Technical University, Ankara, Turkey

Correspondence
Gulum Sumnu, Department of Food Engineering, Middle East Technical University, Ankara 06800, Turkey.
Email: gulum@metu.edu.tr

Abstract

Although glutaraldehyde (GLU) has been frequently preferred to improve some characteristics of bio-degradable food packages, it is regarded as a hazardous chemical. Therefore, in this study, the possibility of replacement GLU with citric acid (CA) a non-toxic compound was questioned in a film formation. Different ratios of GLU and CA on faba bean flour, chitosan, and curcumin film were examined. To determine the most favorable film composition, water solubility (WS), swelling degree (SD), water contact angle (WCA), water vapor permeability (WVP), and mechanical properties of the films were examined. In addition, the effects of crosslinking agent and their ratios on crystallinity (XRD), thermal properties (DSC and TGA), and antioxidant activity (DPPH and ABTS) were also studied. Time Domain Nuclear Magnetic Resonance (TD- NMR) relaxometry was also employed to explain distribution and mobility of the protons in faba bean flour, chitosan, and curcumin films. At the end of the analysis, it was concluded that CA and GLU reduced SD by 75% and 13% compared to the films without cross-linker, respectively. Incorporation of crosslinking agent increased the WCA from 77.22° to 99.41° and caused formation of more hydrophobic surfaces. Increasing both crosslinking ratios restricted the permeance drastically which was more than 110%. Furthermore, the lowest WVP was measured for the films containing CA at 1.5% w/v ratio (FC-1.5C). While GLU improved the tensile strength (TS) of the film, lower elongation of the films caused formation of brittle character which limited the utilization of the films. At the end of the analysis, it was concluded that FC-1.5 had more feasible character with respect to the other films and CA was suggested as a crosslinking agent instead of GLU for faba bean-chitosan films.

KEYWORDS
active food package, chitosan, citric acid, crosslinking, curcumin, faba bean, glutaraldehyde, NMR

1 | INTRODUCTION

Nowadays, biodegradable and eco-friendly components have drawn attention because of increasing environmental concerns originated from petroleum-based packaging materials. In this sense, to replace traditional packaging, natural biopolymers such as polysaccharides, proteins, and lipids have been regarded as possible alternatives (Lin et al., 2019).

Because flours contain carbohydrates, lipid, and protein together, they have been an excellent source for producing food packages. For example, banana flour mixed with chitosan (Pitak & Rakshit, 2011), rice flour combined with fish gelatin (Ahmad et al., 2015), and quinoa flour (Pagno et al., 2016) have been studied to serve as possible food package alternatives. Among different flour types, faba bean, also known as broad bean, filed bean, and horse bean (Multari et al., 2015), is a good source of protein and carbohydrate. The protein content of faba bean is higher than other high protein flours such as pea flour (Yildiz, Bayram, et al., 2021) and lentil flour (Aydogdu et al., 2019). In addition to that, faba bean contains high amount of secondary metabolites, that is, phenols and flavonoids that enrich their antioxidant activity (Millar et al., 2019). However, film formation performance of faba bean flour has not been studied yet.

Chitosan, a natural polysaccharide obtained from chitin, is one of the most commonly used biopolymer for food packaging applications owing to its non-toxicity, biodegradability, biocompatibility, and antioxidant activities (Yujia Liu et al., 2016). However, the hygroscopic nature of chitosan affects both swelling and permeability characteristics of the chitosan films adversely (Pavoni et al., 2021).

Although films made from polysaccharides show good oxygen and carbon dioxide barrier properties due to their tightly packed network structure, they are generally permeable to water vapor due to their hydrophilic nature (Mohamed et al., 2020). On the other hand, proteins provide better mechanical features to the produced films compared to polysaccharides. However, the hydrophilic nature of proteins also leads to poor water vapor barrier characteristics with the films (Mohamed et al., 2020). To eliminate potential drawbacks of these biopolymer films, crosslinking these compounds to modify film structure is one of the promising solutions.

For example, sodium trimetaphosphate (STMP) (Aydogdu et al., 2020) and sodium sulphate crosslinking agents (Kalaycıoğlu et al., 2017) were used in guar gum/orange oil emulsion and chitosan antimicrobial film, respectively. Further, the effect of graphene oxide (Grande et al., 2017) on crosslinking chitosan films and UV induced crosslinking (Zhou et al., 2008) on corn starch films were also analyzed.

Rather than these crosslinking agents, citric acid (CA) is a bio-based tricarboxylic acid and is commonly used due to its low-cost, non-toxic nature. The carboxyl group of citric acid might react with the hydroxyl and amino group of different biopolymers (Nataraj et al., 2018; Yang et al., 2010). Thus, CA was utilized to improve swelling, mechanical, and gas barrier properties of many films such as potato starch/chitosan (Wu et al., 2019), cassava starch (Seligra et al., 2016) poly (vinyl alcohol)/starch/graphene (Jose & Al-Harthi, 2017), and wheat straw hemicellulose (Azeredo et al., 2015).

On the other hand, glutaraldehyde is one of the most commonly preferred crosslinking agents for proteins and polyhydroxy compounds. Because it has a rigid chemical structure without any hydrophilic group, the addition of glutaraldehyde decreases the water sensitivity of the material. The carbonyl group of glutaraldehyde reacts with the amino group (chitosan) and hydroxyl group of polysaccharide molecules (Gonenc & Us, 2019).

Curcumin is one of the most valuable ingredients in turmeric and has been long used in different fields due to its anticancer, antioxidant, antimicrobial, and anti-arthritic character (Gutierrez-Gonzalez et al., 2020). Antioxidant activities of curcumin were attributed to electron donor ability to neutralize free radicals by producing stable products. Furthermore, studies shown that scavenging hydrogen peroxide ability of curcumin was higher than α-tocopherol, butylated hydroxyanisole (BHA), and butylated hydroxytoluene (BHT), most commonly used antioxidants in food science. However, BHA and BHT were to blame for carcinogenesis and liver damage (Ak & Gülçin, 2008). Therefore, taking advantage of using natural and safer antioxidants has become more promising in food packages.

Although it is a well-known fact that glutaraldehyde is a toxic chemical, it is still frequently used as a crosslinking agent in food packaging applications. In this perspective, it was aimed to compare the performance of different crosslinking agents in the production of curcumin added active film. The solubility, water vapor permeability, mechanical property, thermal property, antioxidant activity, and contact angle of the films were studied. Furthermore, the films were also compared in terms of crystallinity, distribution, and mobility of the protons to interpret the different crosslinking agents and ratios.

2 | MATERIALS AND METHODS

Curcumin (1,7-bis [4-hydroxy-3-methoxyphenyl]-1,6-hepadiene-3,5-dione), medium molecular weight (75–85% deacetylated) chitosan, ABTS, glycerol, and ethanol were purchased from Merck (Darmstadt, Germany). Sodium carbonate, Folin–Ciocalteu reagent, 2,2-diphenyl-1-picrylhydrazyl, and acetic acid were purchased from Sigma-Aldrich. Faba bean flour containing (weight basis) 29% protein, 30% carbohydrate, 2.4% fat, citric acid, and glutaraldehyde (50%) were purchased from Havancızade Gıda (İstanbul, Turkey), Smart Kimya (İzmir, Turkey), and Alfasol, respectively.

2.1 | Film preparation

Chitosan (2% w/v) was dissolved in acetic acid solution (2% v/v) overnight at 45°C by using a magnetic stirrer at 750 rpm (MaxTir 500, Daihan Scientific, Seoul, Korea). A slurry of faba bean flour (4%, w/v) was prepared by stirring at 750 rpm and at 80°C for 45 min to complete starch gelatinization and protein denaturation. After cooling down the slurry to 45°C, chitosan and flour slurry were mixed in equal

volumes. Then, 0.4% (w/v) glycerol was added to the solution as a plasticizer. Curcumin (5% w/v) was dissolved in ethanol and 1 ml of this solution was added into the mixture and film-forming solution (FFS) was obtained. Films without any crosslinking agent were regarded as a control (FC-C). To prepare citric acid (CA) cross-linked films (FC-0.5C, FC-1C, FC-1.5C), CA was added to the FFS in different ratios (0.5%w/v, 1% w/v, 1.5% w/v). To obtain glutaraldehyde (GLU) (FC-30GLU, FC-60GLU, FC-120GLU) cross-linked films, GLU was included in to the FFS in different ratios (0.03% v/v, 0.06 v/v, and % 0.12 v/v). Films were symbolized according to the presence of crosslinking agents and ratio. The nomenclature was given in Table 1. FFS was stirred at 1,200 rpm for 45 min and then degassed using an ultrasonic bath (Lab Companion, Jeiotech, Seoul, Korea) at 37 kHz for 25 min. Solutions of 15 g were poured into LDPE Petri plates and dried in a 55°C oven (Binder ED 115, Tuttlingen, Germany) for 6.5 h. Films were kept in a climate chamber at a constant relative humidity of 52% before analysis.

2.2 | Moisture content, swelling degree, and water solubility of the films

MC, SD, and WS of the films were measured with the method described by Wu et al. (2019). First, the films were cut into pieces (2 cm × 2 cm), and their initial weight was recorded (W1). Then, the films were dried in 105°C oven until reaching a constant weight (W2).

After that, they were immersed in 25 ml of distilled water at room temperature for 24 h. After removal, the excess water on the surface was removed by the filter paper, and the films were weighed again (W3). Finally, they were dried in a 105°C oven for 24 h, and the last weight was recorded (W4). Moisture content, swelling degree, and water solubility of the films were calculated by using Equations 1–3 below:

$$\text{Moisture content (MC)}\,(\%) = \frac{W_1\text{-}W_2}{W_1} \times 100 \quad (1)$$

$$\text{Swelling degree (SD)}\,(\%) = \frac{W_3\text{-}W_2}{W_3} \times 100 \quad (2)$$

TABLE 1 Nomenclature of the faba bean flour-chitosan-curcumin films (FC)

Nomenclature	Citric acid (CA) % (w/v)	Glutaraldehyde (GLU) % (v/v)
FC-C	-	-
FC-0.5C	0.5	-
FC-1C	1.0	-
FC-1.5C	1.5	-
FC-30GLU	-	0.03
FC-60GLU	-	0.06
FC-120GLU	-	0.12

$$\text{Water solubility (WS)}\,(\%) = \frac{W_2\text{-}W_4}{W_2} \times 100 \quad (3)$$

2.3 | Water contact angle

The surface hydrophobicity of the films was analyzed by a goniometer (Attension Theta, Sweden). A drop of distilled water was placed on the surface of the films (4 cm^2), and static contact angle was measured.

2.4 | XRD

Crystalline properties of the films were analyzed by X-ray diffractometer (Rigaku Ultima-IV, USA) using copper (Cu) irradiation with 30 mA current and 40 kV energy. Samples were scanned at an angular range of 5° and 70° scanning range with 2°/min scanning rate.

The crystallinity degree of the samples was determined by using Equation 4, based on the method described by Demirkesen, Campanella, Sumnu, Sahin, and Hamaker (2014).

$$\text{Total Crystallinity}\,(T_C) = \frac{I_c}{I_c + I_a} \quad (4)$$

where I_c is integrated intensity of crystalline phase and I_a is the integrated intensity of amorphous phase.

2.5 | Water vapor permeability

To measure water vapor permeability (WVP) of the films, the method described by Yildiz, Bayram, et al. (2021) was used. First, the thickness of the films was measured from different random points with a digital micrometer (LYK 5202, Loyka, Ankara, Turkey). Then, the cylindrical test cups with 40 mm internal diameter were filled with 35 ml water. After placing the films between cup and cap, it was screwed. The cups' initial weight was recorded and placed in a desiccator which was equilibrated to nearly 0% RH by using silica gels. The weight change of the cups was recorded through a 12-h period at 1 h intervals. The relative humidity and temperature in the desiccator were controlled by using a humidity/temperature logger (EBI20-TH1, EBRO, Ingolstadt, Germany). Finally, WVP of the films were calculated using the Equation 5 below:

$$\text{WVP} = \frac{WVTR \times (\Delta x)}{\left(\frac{R_1 - R_2}{100}\right) \times P_{sat}}. \quad (5)$$

Water vapor transmission rate (WVTR) can be calculated from weight changes versus time graph (g m^{-2} s^{-1}). R1 and R2, respectively, represented relative humidity inside and outer sides of the cups. Δx is the thickness of the films (m). Finally, the Psat (Pa) is the saturated water vapor pressure at room temperature.

2.6 | Differential scanning calorimetry

Thermal analysis of chitosan, curcumin, faba bean flour, and films was performed by using a differential scanning calorimeter (Pyris 6 DSC, PerkinElmer, Massachusetts, USA) with a method described by Yildiz, Sumnu, and Kahyaoglu (2021). About 5 mg was placed in an aluminum pan and heated with a heating rate of 10°C/min from 25°C to 350°C.

2.7 | Thermogravimetric analysis

Thermogravimetric analysis of the chitosan, curcumin, faba bean flour, and films were carried out using a thermo-gravimetric analyzer (Perkin Elmer Pyris 1) with a method described by Yildiz, Sumnu, and Kahyaoglu (2021). Sample of 5 mg was heated from 30°C to 600°C at a rate of 10°C/min and nitrogen flow rate of 30 ml/min.

2.8 | Mechanical properties

Tensile strength, Young's modulus, and percentage elongation at break were measured by a texture analyzer (Brookfield, Ametek CT3, Mid- dleboro, MA, USA, TA- DGA tension probe). The test was carried out with using 0.4 N load cell at a test speed of 0.40 mm/s.

2.9 | Antioxidant activity

2.9.1 | DPPH radical-scavenging activity

To determine the DPPH radical-scavenging activity, a method given by Yildiz, Bayram, et al. (2021) with some modifications was used with some modifications. Films (~0.0245 g) were dissolved in 15 ml ethanol: water (80:20) solution and centrifuged at 1,500*g* for 20 min. Then, a diluted sample of 2 ml was mixed with 2 ml DPPH (2,2-diphenyl-1-picrylhydrazyl) solution. Absorbance value of samples was measured at 517 nm after 30 min. DPPH scavenging activity of the samples was calculated according to Equations 6 and 7 below:

$$\text{DPPH scavenging activity}\,(\%) = \frac{A_{control} - A_{sample}}{A_{control}} \times 100. \quad (6)$$

$A_{control}$ and A_{sample} are the absorbance of the DPPH solution with and without sample.

2.9.2 | ABTS radical scavenging activity

To prepare the ABTS analysis, potassium persulfate (2.6 mM) and ABTS (7 mM) were mixed and stored at room temperature in the dark. The diluted sample of 0.5 ml was mixed with 1.5 ml ABTS solution and incubated at room temperature for 30 min. The absorbance of the solution was measured by a spectrophotometer at 734 nm (Roy & Rhim, 2020). ABTS scavenging activity of the samples was calculated according to the equations below:

$$\text{ABTS scavenging activity}\,(\%) = \frac{A_{control} - A_{sample}}{A_{control}} \times 100. \quad (7)$$

$A_{control}$ and A_{sample} are the absorbance of the ABTS solution with and without sample.

2.10 | Time domain NMR relaxometry

Time domain (TD) NMR relaxometry was carried out to interpret the distribution and mobility of protons including crystallinity, crosslinking, and polymer-water interactions. The method of this analysis was adopted from Ilhan et al. (2020).

TD NMR relaxometry experiments were conducted on a 0.5 T NMR system (Spin Track, Resonance Systems GmbH, Kirchheim/Teck, Germany) operating at a ^{1}H of 20.34 MHz. For spin–spin relaxation time (T_2) measurements, Carr-Purcell- Meiboom-Gill (CPMG) sequence was used with 60 us echo time, 50–70 echoes depending on the sample. Relaxation period (TR) were chosen as 8,000 ms, and 16 scans were acquired for T_2 measurements. Non-Negative-Least-Square (NNLS) analysis was conducted on T_2 curves to obtain a relaxation spectrum using PROSPA (Magritek, New Wellington, New Zealand).

For spin–lattice time (T_1) measurements, saturation recovery sequence having observation time changing between 250 and 350 ms and 16 scans. Mono-exponential fitting was conducted on the relaxation curves using MATLAB.

2.11 | Statistical analysis

All measurements were carried out in two replicates and reported as means with standard errors. Statistical analysis of results was done by analysis of variance (ANOVA) with using the general linear model tool of Minitab (version 16, State College, PA, USA). For the comparison of results, Tukey's comparison test was used ($p \leq 0.05$). To explain the effects of independent variables on the film characteristics, one-way model was used.

3 | RESULTS AND DISCUSSION

3.1 | Physical properties of FC films

The main aim of the crosslinking in biopolymer films was to decrease solubility and swelling for the improvement of water resistance and applicability. The solubility of the FC films was significantly lower than the films with similar compositions (Table 2). For example, the solubility of lentil flour (Aydogdu et al., 2018), pea flour (Yildiz, Bayram, et al., 2021), and rice flour (Vargas et al., 2017) based films

were between 25% and 42%. The main reason for this result might be the bond formation between the hydroxyl group of starch, amino groups of chitosan (Figure S2). This might decrease the water affinity, which resulted in even a further decrease in water solubility of the FC films without any cross linker (Bajer et al., 2020). While the amide group of chitosan might function as a proton acceptor, the hydroxyl group of starch might behave as a weak proton donor. Therefore, the formation of hydrogen bonding became more favorable (Sudhakar, Sowmya, Selvakumar, & Bhat, 2012). Furthermore, the presence of curcumin might have a decreasing effect on water solubility due to its hydrophobic nature (Roy & Rhim, 2020).

The addition of both crosslinking agents caused a decreasing trend in water solubility (Table 2). The hydrophobic ester bond formation between CA and polysaccharides (Figure S3a) lowered the number of available hydrophilic hydroxyl groups and, in turn, decreased the solubility of the films (Wu et al., 2019). Similarly, the less available amino group of chitosan resulted in less soluble films (Figure S4a). However, only CF-1.5C films had significantly lower solubility than the control films. The main reason for that might be the higher crosslinking density of the CF-1.5C films.

Although chitosan is a polysaccharide, unlike many other biopolymers, it is insoluble in water. It dissolves in weakly acidic solutions and forms hydrogels. Since the hydrogels can absorb a high amount of water, this feature makes application chitosan-based films practically useless (Murray & Dutcher, 2006). Therefore, to prevent such an outcome, crosslinking of chitosan films becomes more critical. The main idea behind the crosslinking is to reduce the free volume by increasing the number of junctions and thereby restrict the possible hydrogen bond formation between chitosan and water molecules (Wu et al., 2019).

The swelling degree of all the films decreased drastically with increasing the ratio of the crosslinking agents (Table 2). Glutaraldehyde has three hydroxyl groups, while citric acid has three carboxyls and one hydroxyl group in the structure (Figure S1c,d). This means that citric acid has a higher chance to make covalent bonds as compared to glutaraldehyde. Therefore, the lowest amount of citric acid reduced swelling degree more than the highest amount of glutaraldehyde (Yoon, Chough, & Park, 2006).

Moisture content was expected to decrease in the crosslinked films; however, it had an increasing trend with the addition of the crosslinkers. Although GLU and CA reduced the starch and chitosan hydrophilic sides, both crosslinking agents might have unreacted hydroxyl or carbonyl groups. Because all the crosslinked molecules were bulky, steric hindrance might be the restrictive factor and the reason for unreacted groups. Therefore, water molecules might have attached to these available groups through hydrogen bonding and increased the moisture content of the crosslinked resulting films.

The surface hydrophilicity and hydrophobicity were determined by water contact angle where $\theta > 65^\circ$ indicated hydrophobic surfaces (Narasagoudr et al., 2020). In the literature, the water contact angle of neat chitosan film was reported nearly as 103° (Silva et al., 2007). Although faba bean flour increased surface wettability, FC films still had highly hydrophobic surfaces whose water contact angles were between 73° and 99° (Table 2). These findings were attributed to the strong covalent bonding between starch and chitosan (Zhao et al., 2018). Furthermore, as mentioned, curcumin is a hydrophobic substance. It might also influence the surface contact angle of the films. Similarly, in the study of Musso et al. (2017), it was reported that the addition of curcumin to gelatin films led to increasing hydrophobic character of the films without affecting water solubility. In addition, chitosan–potato starch citric acid cross-linked films had significantly lower water contact angles which were in the range of 34° and 57° as compared to FC films (Wu et al., 2019). It should be noted that the films' water contact angle and swelling degree were inversely related to each other with a correlation coefficient of −0.948 ($p = 0.000$). The reduction of available hydrophilic sides and denser structure of the film increased hydrophobicity. In addition, crosslinking reactions might have changed the surface roughness of films which caused larger contact angles because of heterogeneous wetting (Wu et al., 2019).

3.2 | Water vapor permeability

Water vapor permeability (WVP) of the films was shown in Table 2. WVP of FC films was dependent on many factors such as crystalline-

TABLE 2 WS, SD, MC, WCA, and WVP of faba bean–chitosan curcumin cross-linked films

	WS (%)	SD (%)	MC(%)	WCA (°)	WVP (10^{-11}) ($g\ m^{-1}\ s^{-1}\ Pa^{-1}$)
FC-C	22.98 ± 0.39^{a}	136.58 ± 3.83^{a}	9.52 ± 0.56^{d}	73.22 ± 0.59^{d}	42.55 ± 9.01^{a}
FC-0.5C	21.16 ± 1.04^{ab}	69.74 ± 4.84^{c}	10.37 ± 0.38^{cd}	86.21 ± 1.54^{bc}	0.34 ± 0.02^{c}
FC-1C	21.93 ± 0.23^{ab}	46.77 ± 2.10^{d}	12.25 ± 0.24^{bc}	94.36 ± 0.02^{ab}	0.47 ± 0.02^{b}
FC-1.5C	17.35 ± 1.20^{b}	33.63 ± 4.37^{d}	12.20 ± 0.68^{bc}	99.41 ± 0.28^{a}	0.29 ± 0.00^{c}
FC-30GLU	22.40 ± 1.14^{ab}	126.11 ± 3.56^{ab}	15.52 ± 0.40^{a}	78.54 ± 5.80^{cd}	27.44 ± 0.72^{a}
FC-60GLU	20.51 ± 2.20^{ab}	128.47 ± 1.36^{ab}	12.21 ± 1.02^{bc}	79.02 ± 3.17^{cd}	0.32 ± 0.02^{c}
FC-120GLU	18.42 ± 2.022^{ab}	117.05 ± 3.44^{b}	12.99 ± 0.92^{b}	82.67 ± 0.36^{cd}	0.30 ± 0.00^{c}

Note: Columns having different letters are significantly different ($p \leq 0.05$). WS, SD, MC WCA, and WVP referred to water solubility, swelling degree, water contact angle, and water vapor permeability of the films, respectively.

amorphous ratio, hydrophilic- hydrophobic ratio, the integrity of the film, polymer chain mobility (Balasubramanian et al., 2018), solubility in water, and moisture content. Therefore, the permeability was shaped under multiple effects, not based on a single parameter. For example, moisture affected the intermolecular forces between polymer chains by increasing free volume and enhancing chain mobility (Yeamsuksawat & Liang, 2019). Thus, films with higher moisture content were expected to have higher permeability. Because molecule alignments were more compact and regular in the crystalline region compared to the amorphous part, transferring rate of water molecules from one side to the other became relatively slow (Uygun et al., 2020). Furthermore, higher WCA could be interpreted as a reduction in potential interaction between water vapor and film surface. Therefore, films with higher WCA were expected to have lower WVP.

As seen in Table 2, the addition of crosslinking agents to the films caused a decreasing trend in WVP. However, WVP of FC-30GLU was not significantly different than that of FC-C. At that point, it should be noted that FC-30GLU achieved the highest moisture content, and this might be effective on their WVP. It might be concluded that during WVP measurement, exposing films to 100% RH might lead to modification of film matrix and thereby increased the permeability. Although solubility values of FC-1C were not different than control films (Table 2), it had moderately high water contact angles and relatively low swelling degrees. Under these effects, WVP of FC-1C received highest permeability after FC-C and FC-30GLU. Finally, as expected crosslinking agents formed a more compact network by increasing compatibility. This resulted in not only reduction in the polarity of all components (Figure S5a,b; Sun et al., 2018), but also decreasing in permeability.

3.3 | Mechanical properties

Enhancement in TS was generally expected with introducing crosslinking agents due to increasing and tightening molecular interactions. As shown in Table 3, although GLU addition resulted in increasing TS of the film, incorporation of citric acid decreased TS. Increasing TS might be interpreted as more resistance to mechanical stress. On the other hand, increasing EAB was the indicator of the higher stretchability and more deformable films. High TS and low EAB were the indicators of brittle materials as in the example of GLU incorporated films. This showed that the motion of FC film matrices was more restricted after incorporation of GLU. Similar findings were also reported in the study of gelatin films cross-linked with GLU (Martucci et al., 2012).

On the other hand, FC-1C and FC-1.5C films showed a yield-like deformation similar to the thermoplastic films with lower TS and high EAB. As can be seen, after an elastic deformation, a large deformation region was observed, which indicated enhancement of ductility and extensibility (Martucci et al., 2012). Although in this study, CA was preferred as a crosslinking agent, some studies also reported plasticizer character of unreacted CA at high ratios by reducing the interaction between components (Wu et al., 2019).

The present research showed that both effects might coexist, although these impacts seemed to be inconsistent with each other. TS of FC-1C and FC-1.5C films tended to decrease more than 30% compared to FC-C. EAB of FC-1C (4.23 $\pm$ 0.66%) and FC-1.5C (12.93 $\pm$ 1.06%) films were also significantly different than the FC-C (1.67 $\pm$ 0.30%). Therefore, it might be concluded that citric acid played a role as a plasticizer for the mechanical properties of the films. On the other hand, especially for the FC-1.5C films, WS, SD, and WVP significantly decreased, reflecting the behavior of the crosslinking agent. Similar outcomes were also reported in the study of Azeredo et al. (2015) and Sebti et al. (2003).

These controversial outcomes were also explained by the higher heterogeneity of the spacing between cross-links (Sebti et al., 2003). This heterogeneity might distribute the stress on the chains, which were not stabilized by H— bonding. After non-H— bonding chains had been broken, they transferred the stress to the other chains by forcing them to either break or slip to release the stress.

Although high TS was desirable for the packaging films, stretchability was another important character for the film application. Therefore, GLU incorporated films with high TS, but low elongation and rigid structure restrict its application as a packaging material. On the other hand, lower TS and higher EAB of CA cross-linked films were more feasible in practice.

TABLE 3 Mechanical and thermal properties of faba bean chitosan crosslinked films

	TS (MPa)	EAB (%)	Melting onset(°C)	Melting peak(°C)	Melting end(°C)	Melting Elthalpy(J/g)
FC-C	12.67 ± 0.08^{c}	1.67 ± 0.30^{c}	169.46 ± 0.77^{a}	173.67 ± 1.58^{a}	187.43 ± 1.23^{bc}	104.43 ± 2.05^{c}
FC-0.5C	9.04 ± 1.01^{d}	1.25 ± 0.57^{c}	173.56 ± 1.0^{a}	177.81 ± 1.40^{a}	191.64 ± 0.69^{b}	112.71 ± 1.28^{b}
FC-1C	8.62 ± 0.21^{d}	4.23 ± 0.66^{b}	171.22 ± 1.6^{a}	176.23 ± 1.79^{a}	193.54 ± 1.03^{b}	167.10 ± 1.52^{a}
FC-1.5C	7.15 ± 0.30^{d}	12.93 ± 1.06^{a}	173.05 ± 1.46^{a}	178.92 ± 1.54^{a}	200.10 ± 2.65^{a}	201.87 ± 1.69^{a}
FC-30GLU	14.61 ± 0.31^{c}	2.61 ± 0.48^{bc}	169.1 ± 0.42^{a}	172.83 ± 1.2^{a}	185.17 ± 1.20^{c}	102.81 ± 1.34^{c}
FC-60GLU	21.96 ± 0.73^{a}	2.43 ± 0.17^{bc}	173.22 ± 1.66^{a}	178.05 ± 2.83^{a}	193.24 ± 1.72^{b}	92.87 ± 2.19^{d}
FC-120GLU	19.28 ± 0.06^{b}	1.71 ± 0.11^{c}	174.95 ± 2.87^{a}	179.23 ± 1.14^{a}	192.26 ± 1.76^{b}	102.54 ± 1.97^{c}

Note: Columns having different letters are significantly different ($p \leq 0.05$).

3.4 | Thermal properties

The weight loss versus temperature curve of films, chitosan, faba bean flour, and curcumin was shown in Figure 1. In general, the thermal decomposition of FC films followed multistep decomposition. The first step centered at 100°C was due to the evaporation of water and other volatile compounds. The second stage degradation appeared around 200°C was because of evaporation of glycerol (Bagheri et al., 2019). Furthermore, for CA cross-linked films, evaporation of citric acid derivatives also overlapped at these values (190–200°C; Qiao et al., 2021). This was followed by a decomposition process which was the highest weight loss observed for all samples. This step corresponded to the depolymerization and decomposition of acetylated and deacetylated units of the polymer (Wu et al., 2019), in other words, cleavage of covalent bonds formed during crosslinking between starch, protein and chitosan (Sharma et al., 2018). Although the peak temperature of this stage generally was positioned around 300°C, this stage shifted gradually to higher temperatures (nearly 315°C) with the increasing CA ratio in films which was the indicator of the strong intermolecular interactions between components. However, the degradation temperature of GLU incorporated films had a similar decomposition peak temperature to FC-C, which was located approximately at 290°C.

Differential scanning calorimetry results of all films were shown in Table 3. All films exhibited an endothermic peak between 170°C and 180°C. XRD analysis showed that crosslinking agents had a decreasing impact on the crystallinity of the films (Table 3). Therefore, it was expected the reduction in Tm and melting enthalpy (ΔHm; Jose & Al-Harthi, 2017). On the other hand, it was reported that introducing cross-linker slightly increased melting temperature by stabilizing bond between all components (Sharma et al., 2018). In addition to that, crosslinking agents increased molecular weight of polymeric matrix through intermolecular interactions (Sharma et al., 2018). Therefore, under two counteracting effects, reduction of crystallinity and stabilizing bond strength, Tm did not change significantly. Although the melting enthalpy of GLU cross-linked films nearly the same as FC-C, CA-introduced films exhibited a noticeable increase in the melting enthalpy with an increasing CA ratio. In addition to bond stabilizing effect, melting of CA in the films might also have an effect on increasing enthalpy because the melting temperature of CA (~190°C) overlapped the Tm of the films (Shafie et al., 2019).

3.5 | Antioxidant activity

FC-C films showed the highest DPPH and ABTS activity because of curcumin and the active antioxidant biopolymer, chitosan. The hydroxyl and amino groups of chitosan interacted with free radicals and exhibited the radical scavenging activity (Roy et al., 2021). In addition to this, antioxidant activity of curcumin was originated from phenolic hydroxyl group and methylene group of β-diketone moiety (Priyadarsini et al., 2003).

As can be seen in Table 4, the addition of cross-linking agent decreased the antioxidant activity of the films by nearly 50%. First, the cross-linking reaction might be responsible for this result. Carboxyl group of CA and GLU might have reacted with the hydroxyl and amino group of chitosan and active sides of curcumin during cross-linking reaction causing a decrease in the number of active sides required for the antioxidant activity. In addition to that, releasing of the active agent, curcumin was inversely correlated with the cross-linking degree. Because the releasing rate was expected to be lower in the cross-linked polymer matrix, cross-linked films achieved relatively lower antioxidant activity (Valizadeh et al., 2019).

In parallel with this finding, releasing of active components was also linked to the swelling degree of polymer matrix (López de Dicastillo et al., 2016). As shown in Table 2, the highest swelling degree was observed for FC-C, as well as the highest DPPH and ABTS activity.

Although CA incorporated films achieved a relatively lower swelling degree, they showed higher antioxidant activity than GLU. This

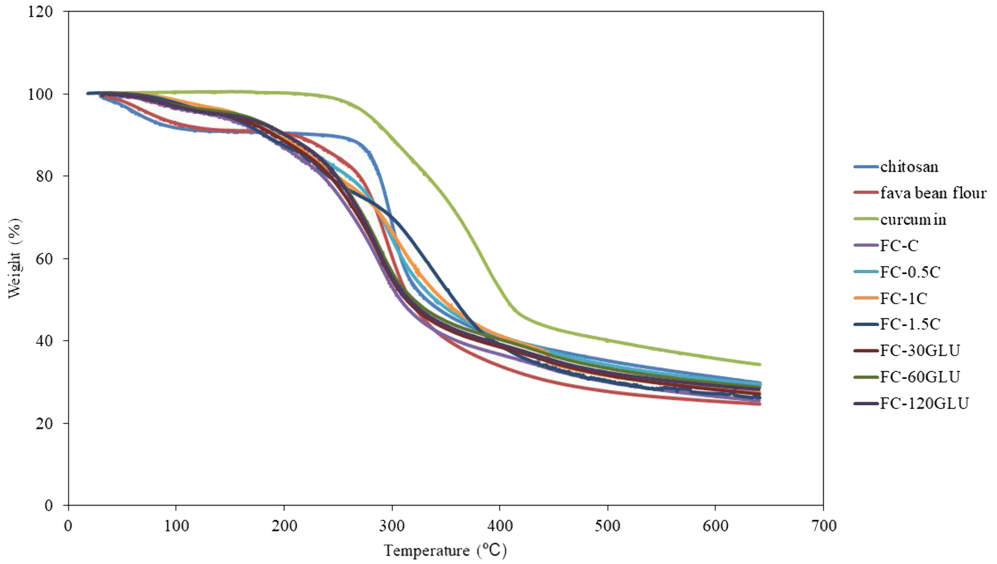

FIGURE 1 TGA curves of FC films

result was probably due to the antioxidant activity contribution of CA (Sauraj et al., 2018).

3.6 | XRD

The relative degree of crystallinity (RDC) was measured by the ratio between area of crystallinity and total area under the XRD diffraction pattern (Liu et al., 2019). RDC and XRD pattern of the all films were shown in Table 4 and Figure 2. There might be two main reasons behind the crystallinity of the FC films. The first one was the retrogradation of starch (Seligra et al., 2016), and the second one was the presence of NH_2 (amine) group in chitosan which promotes the formation of hydrogen bond between polymer chain (Pavoni et al., 2021). Introducing crosslinking agent showed a decreasing tendency on the crystallinity of the films because the carboxyl group of CA and GLU reacted with the hydroxyl and amine groups. Therefore, this interaction restricted the formation of crystal structure in starch and chitosan molecules. As seen, CA added samples had a significantly lower degree of crystallinity compared to FC-C. As mentioned before, CA has more sides to make crosslinking than GLU. Therefore, CA might limit the chain segment movements and thereby interfere with crystallization (Ren et al., 2017).

TABLE 4 DPPH and ABTS activity (%) and RDC of faba bean-chitosan crosslinked films

	DPPH activity (%)	ABTS activity (%)	RDC
FC-C	20.74 ± 1.27^{a}	86.54 ± 1.15^{a}	11.83 ± 1.49^{a}
FC-0.5C	9.40 ± 1.82^{c}	33.01 ± 0.38^{c}	5.15 ± 0.28^{b}
FC-1C	15.20 ± 0.91^{b}	60.80 ± 3.55^{b}	5.85 ± 0.74^{b}
FC-1.5C	11.73 ± 0.01^{bc}	34.57 ± 0.28^{c}	4.96 ± 0.51^{b}
FC-30GLU	10.89 ± 0.16^{c}	27.66 ± 2.87^{c}	13.31 ± 0.41^{a}
FC-60GLU	8.56 ± 0.25^{c}	25.86 ± 1.01^{c}	6.38 ± 0.62^{b}
FC-120GLU	10.29 ± 1.18^{c}	28.20 ± 3.64^{c}	10.38 ± 0.98^{a}

Note: Columns having different letters are significantly different ($p \leq 0.05$).

The characteristic peaks of chitosan were observed around 10° and 20° (2θ). The first peak was the indicator of hydrated crystalline structure because of water molecules attached to the crystal lattice. The peak around 20° (2θ) was attributed to the amorphous part of chitosan (Giannakas et al., 2014). The diffraction peaks around 15.42°, 17°, and 20° (2θ) corresponded to the B-type starch diffraction pattern in faba bean flour (Liu et al., 2013). As seen diffraction pattern of FC films, the intensity of peaks decreased and even some disappeared (15.42°), which was supported by the degree of crystallinity. This

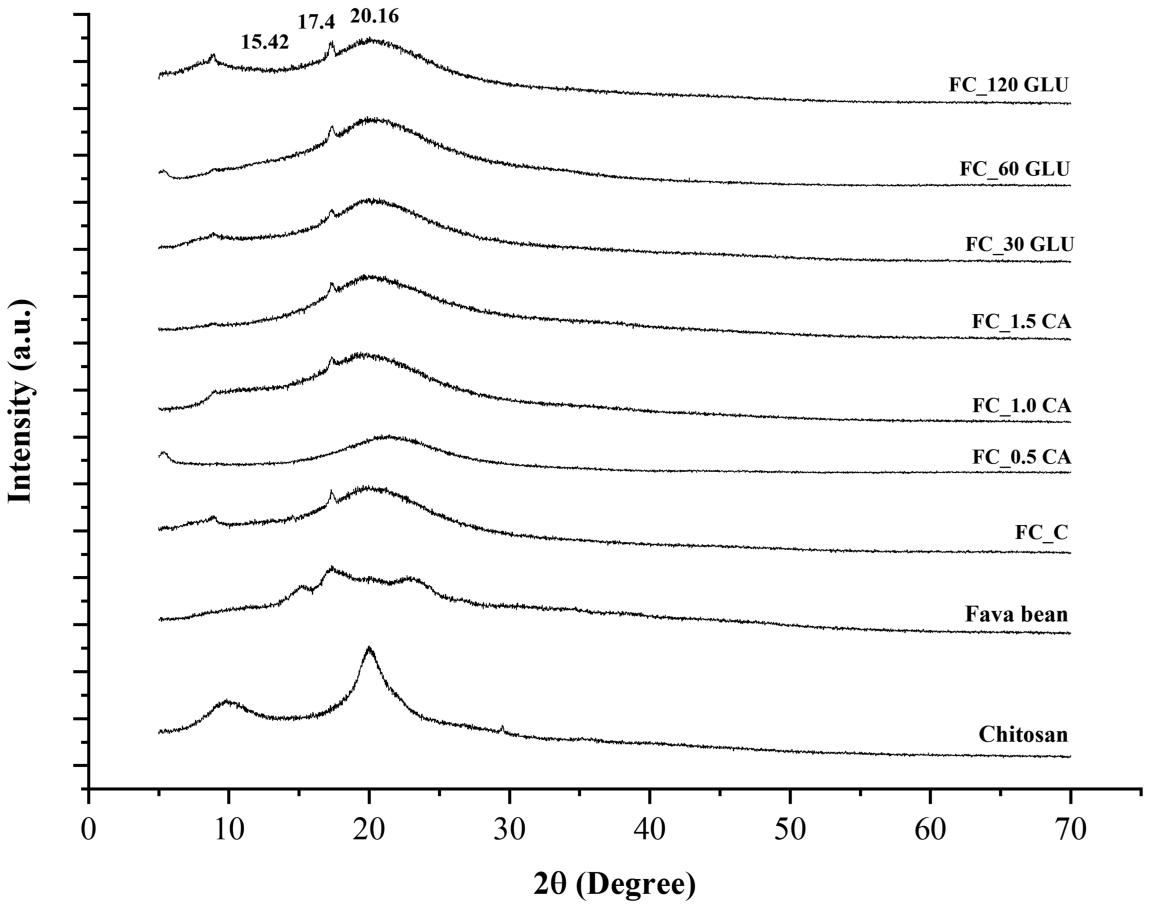

FIGURE 2 X-ray diffraction patterns of the FC films

result showed that interaction between components (starch- chitosan and crosslinking agents) restrained the intramolecular interactions. However, the peak at 17.54° was observed in FC films for all formulations. This peak indicates the formation of a double helical B-type crystalline structure and most sensitive to hydration (Zhong et al., 2011). These results were consistent with the previous research findings related to the amylose and amylopectin films (Myllärinen et al., 2002). It should be noted that although cross-linking decreased the solubility or water sensitivity of the films, the main components of these films were very hydrophilic (chitosan and faba bean). Therefore, a little amount of water interaction or water present in these films (MC) might have an ongoing impact on their structures.

3.7 | Time domain NMR

NMR relaxometry is a noninvasive and user-friendly method preferred to investigate the change in mobile protons of food systems. Because NMR signal is obtained with the contribution of all protons in a sample, it is possible to get insight into the mobility and distribution of different proton compartments, which provides detailed information about the internal structure and complex associations (Ozel, Uguz, et al., 2017; Pocan et al., 2019). It is known that the relaxation times are affected by the presence of free hydroxyl groups; thus, the crosslinking of the films can be detected with the help of differences in the water mobility (Seligra et al., 2016). Therefore, it could be deduced that relaxation times could explain crosslinking, water mobility, or crystallinity of the food products. There are several types of research conducted on the use of relaxation times to characterize proton mobility and distribution on films (Picchio et al., 2018; Seligra et al., 2016; Xiao, 2018). T1, called longitudinal relaxation time, is defined as the time takes for spins to give back energy from the radio-frequency pulse. It is related to the mobility of water protons (Kirtil & Oztop, 2016). Therefore, it could be concluded that the T1 spin–lattice time may provide insight into the moisture content of food products (Le Botlan et al., 1998). The limited movement of the water molecules results in shorter T1 times. Therefore, it can be said that samples with short T1 times had lower water mobility. T1 spin–lattice times of films are given in Figure 3. Results showed that control film (FC-C) had the longest T1 spin–lattice relaxation times, and it decreased as the CA ratio increased, indicating lower water mobility. On the other hand, significant changes were not observed when GLU-containing films were considered. This finding could be explained with the chemical structure of crosslinking agents. Glutaraldehyde has three hydroxyl groups, whereas citric acid has three carboxyls and one hydroxyl group in the structure. It is stated in a study that citric acid added films was better in terms of crosslinking than glutaraldehyde added films due to enhanced inter/intramolecular hydrogen bonding in the presence of carboxyl group and hydroxyl group together (Yoon et al., 2006). Since FC-C films did not contain any crosslinking agents, it was expected to observe the highest water mobility and consequently shorter T_1 spin–lattice times.

It is also worth to mention that in addition to water mobility, information about the crystallinity could be obtained from the spin–lattice relaxation times. According to the study of Le Botlan et al. (1998), longer T_1 relaxation times were associated with the more crystalline regions. When moisture content of the samples were the same, then longer T_1 values might be associated with the effect of crystalline regions (Pocan et al., 2019). According to moisture content measurement, FC-1C, FC-1.5C, FC-120GLU, and FC-60GLU had similar moisture content. When these results were re-evaluated considering the T1 values, it was seen that the FC-1.5 CA sample had the shortest T1 value, indicating lower crystalline regions compare to other films. This outcome was also consistent with the X-ray diffraction experiments because it demonstrates that the total crystallinity of FC-1.5 CA was lower than other films (Table 3).

In addition to spin–lattice time T_1, spin–spin relaxation time T_2 were also measured. T_2, transverse relaxation time, is the time required for transverse magnetization to reach equilibrium value (Ozel, Dag, et al., 2017). It was possible to get insight on the mobility

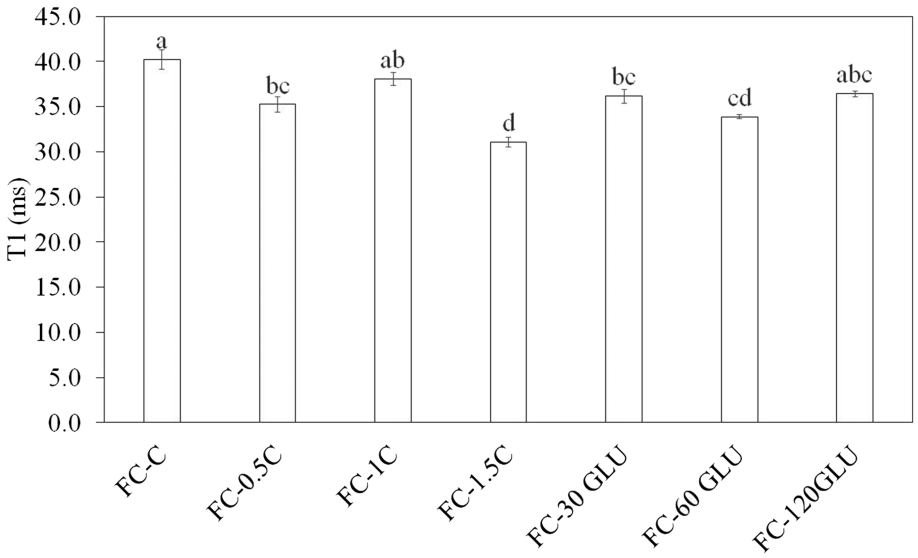

FIGURE 3 T1 spin–lattice times of FC films

of hydrogen molecules depending on length of T2, where short and T2 indicated immobile structure whereas long T2 represented mobile components. Food products generally show multi-compartmental proton distribution, and inverse Laplace transformation can be used to obtain one-dimensional distribution, relaxation spectra, from decaying magnetization curves. To inspect the proton populations in detail, relaxation spectrum analyses were also performed. Representative 1D NMR T2 relaxation spectra of the FC films (Figure 4) showed two distinct proton populations in all FC films. Relative areas (RA) of the corresponding peaks were also given in Table 5.

Depending on the magnitude of T_2 values, slowly relaxing component can be associated with non-exchangeable hydrogen of more mobile subgranular polymer components, whereas fast relaxing component can be ascribed to water molecules trapped in the crystalline phase (Ritota et al., 2008). It was stated that fast transverse relaxation time was dominated by a fast chemical exchange between OH groups

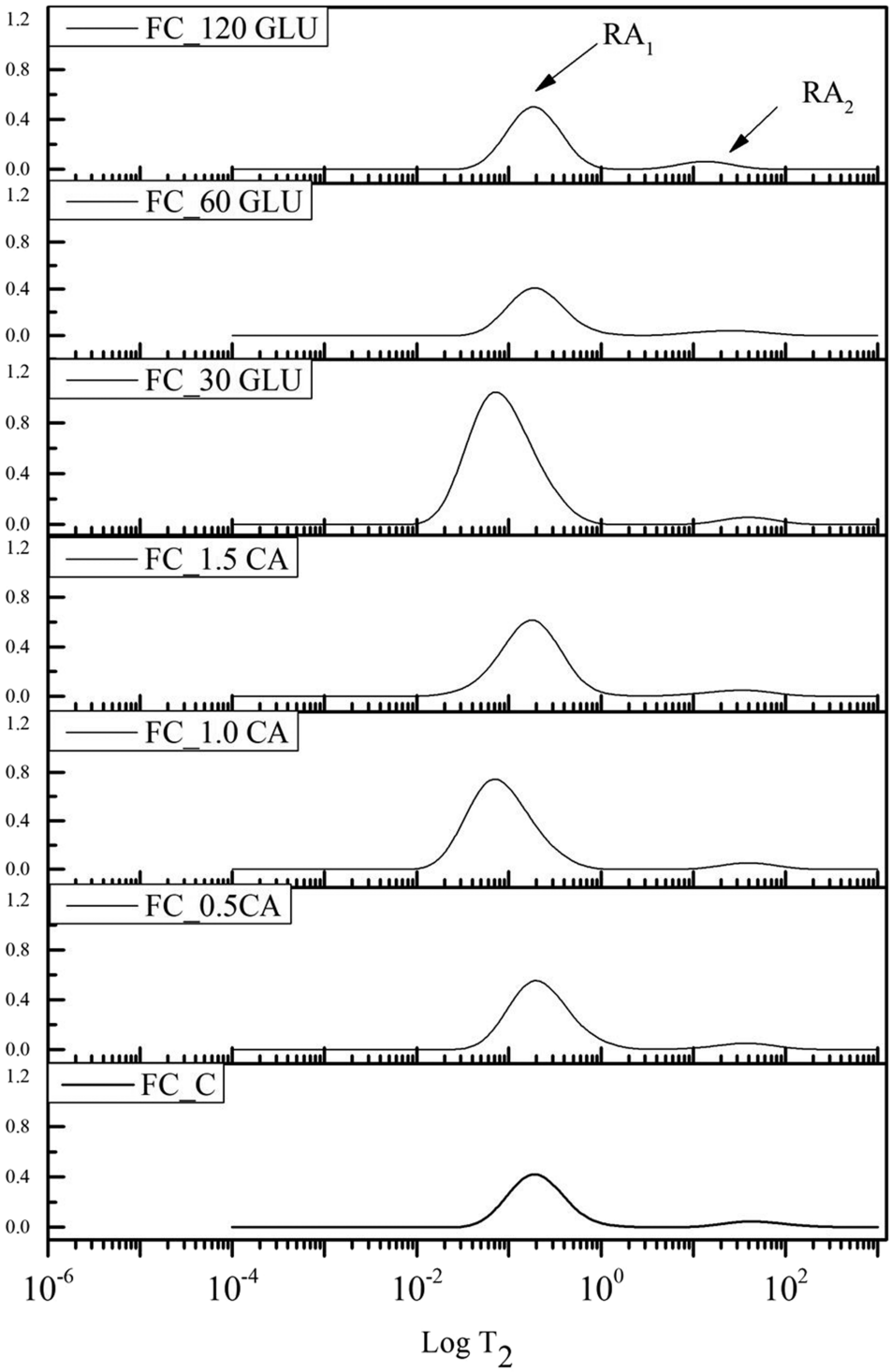

FIGURE 4 ^{1}H NMR relaxation times for all the films

TABLE 5 RA of faba bean–chitosan cross-linked films

	RA_1	RA_2
FC-C	89.06[c]	10.94[a]
FC-0.5 CA	92.07[b]	7.93[b]
FC-1.0 CA	94.67[a]	5.33[c]
FC-1.5 CA	92.37[b]	7.63[b]
FC-30 GLU	96.13[a]	3.87[c]
FC-60 GLU	88.90[c]	11.10[a]
FC-120GLU	88.98[c]	11.02[a]

Note: Columns having different letters are significantly different ($p \leq 0.05$).

of compartments of polymer chain, in other words solid–solid interaction (Ilhan et al., 2020; Ritota et al., 2008). Solid–solid interaction covers both inter and intramolecular interaction of polymers. Therefore, RA1 was shaped under the effect of both starch–starch, chitosan–chitosan (intramolecular–crystallinity), and starch–chitosan (intermolecular–crosslinking). When the results were examined, the relative area (RA) of the first peak of the FC-C and glutaraldehyde containing films (except FC-30 GLU) were lower than the films containing citric acid as the crosslinking agent. As mentioned before, the crystallinity value of FC-30 GLU was the highest according to X-ray diffraction experiments. Based on this, it was hypothesized that the high RA1 might not have been resulted from crosslinking of chitosan starch but from a higher tendency of polymers to interact among themselves.

On the other hand, ascending RA1 with the addition of citric acid might have indicated the enhanced crosslink between chitosan and starch. It is worth noting that, because the second peak is related to water tightly bound to polymers, the decrease in RA2 supports the hypothesis about higher crosslinking between polymers and less interaction with water. Here, it can be concluded that NMR relaxometry and relaxation times might be considered as promising indicator to define quality parameters of films including crystallinity, crosslinking, or water mobility.

4 | CONCLUSION

This study aimed to compare GLU and CA crosslinking performance on faba bean flour–chitosan–curcumin films. Increasing the crosslinking concentration generally improved the film characteristics (WVP and SD) especially for the films containing CA. FC- 30 GLU usually exhibited similar features with the FC-C, particularly WVP and RDC. This might be due to lower crosslinking concentration. On the other hand, CA-1.5C showed advanced attributes including SD, WCA, and WVP. Addition of CA lowered the mechanical strength and brought generally high elongation. However, GLU added films received high TS and lower elongation, which resulted in more brittle character. Antioxidant activity (DPPH and ABTS) of all films was lower than FC-C, which might be related to difficulty in swelling out of curcumin through the film matrix and interaction between crosslinking agents curcumin chitosan. At the end, this might be concluded that FC-1.5C film generally exhibited the most acceptable properties compared to the films with and without a crosslinker. CA might be recommended instead of GLU to improve the film characteristics of water sensitive films. Overall, FC-1.5C films might be suggested as a promising active food packaging material.

CONFLICT OF INTEREST

The authors declare no conflict of interest with any one or any other organizations.

FUNDING INFORMATION

There are no funders to report for this submission.

DATA AVAILABILITY STATEMENT

The data that support the findings of this study are available from the corresponding author up on reasonable request.

ORCID

Eda Yildiz https://orcid.org/0000-0002-1018-9930
Esmanur Ilhan https://orcid.org/0000-0001-5172-9529
Leyla Nesrin Kahyaoglu https://orcid.org/0000-0003-3548-4378
Gulum Sumnu https://orcid.org/0000-0002-2949-4361
Mecit Halil Oztop https://orcid.org/0000-0001-6414-8942

REFERENCES

Ahmad, M., Hani, N. M., Nirmal, N. P., Fazial, F. F., Mohtar, N. F., & Romli, S. R. (2015). Optical and thermo-mechanical properties of composite films based on fish gelatin/rice flour fabricated by casting technique. *Progress in Organic Coatings*, *84*, 115–127. https://doi.org/10.1016/j.porgcoat.2015.02.016

Ak, T., & Gülçin, I. (2008). Antioxidant and radical scavenging properties of curcumin. *Chemico-Biological Interactions*, *174*(1), 27–37. https://doi.org/10.1016/j.cbi.2008.05.003

Aydogdu, A., Kirtil, E., Sumnu, G., Oztop, M. H., & Aydogdu, Y. (2018). Utilization of lentil flour as a biopolymer source for the development of edible films. *Journal of Applied Polymer Science*, *135*(23), 1–10. https://doi.org/10.1002/app.46356

Aydogdu, A., Radke, C. J., Bezci, S., & Kirtil, E. (2020). Characterization of curcumin incorporated guar gum/orange oil antimicrobial emulsion films. *International Journal of Biological Macromolecules*, *148*, 110–120. https://doi.org/10.1016/j.ijbiomac.2019.12.255

Aydogdu, A., Yildiz, E., Aydogdu, Y., Sumnu, G., Sahin, S., & Ayhan, Z. (2019). Enhancing oxidative stability of walnuts by using gallic acid loaded lentil flour based electrospun nanofibers as active packaging material. *Food Hydrocolloids*, *95*(April), 245–255. https://doi.org/10.1016/j.foodhyd.2019.04.020

Azeredo, H. M. C., Kontou-Vrettou, C., Moates, G. K., Wellner, N., Cross, K., Pereira, P. H. F., & Waldron, K. W. (2015). Wheat straw hemicellulose films as affected by citric acid. *Food Hydrocolloids*, *50*, 1–6. https://doi.org/10.1016/j.foodhyd.2015.04.005

Bagheri, F., Radi, M., & Amiri, S. (2019). Drying conditions highly influence the characteristics of glycerol-plasticized alginate films. *Food Hydrocolloids*, *90*(November 2018), 162–171. https://doi.org/10.1016/j.foodhyd.2018.12.001

Bajer, D., Janczak, K., & Bajer, K. (2020). Novel starch/chitosan/aloe vera composites as promising biopackaging materials. *Journal of Polymers and the Environment*, *28*(3), 1021–1039. https://doi.org/10.1007/s10924-020-01661-7

Balasubramanian, R., Kim, S. S., & Lee, J. (2018). Novel synergistic transparent k-Carrageenan/Xanthan gum/Gellan gum hydrogel film: Mechanical, thermal and water barrier properties. *International Journal of Biological Macromolecules*, *118*, 561–568. https://doi.org/10.1016/j.ijbiomac.2018.06.110

Demirkesen, I., Campanella, O. H., Sumnu, G., Sahin, S., & Hamaker, B. R. (2014). A study on staling characteristics of gluten-free breads prepared with chestnut and Rice flours. *Food and Bioprocess Technology*, *7*(3), 806–820. https://doi.org/10.1007/s11947-013-1099-3

Giannakas, A., Grigoriadi, K., Leontiou, A., Barkoula, N. M., & Ladavos, A. (2014). Preparation, characterization, mechanical and barrier properties investigation of chitosan-clay nanocomposites. *Carbohydrate Polymers*, *108*(1), 103–111. https://doi.org/10.1016/j.carbpol.2014.03.019

Gonenc, I., & Us, F. (2019). Effect of Glutaraldehyde crosslinking on degree of substitution, thermal, structural, and physicochemical properties of corn starch. *Starch/Staerke*, *71*(3–4), 1–10. https://doi.org/10.1002/star.201800046

Grande, C. D., Mangadlao, J., Fan, J., De Leon, A., Delgado-Ospina, J., Rojas, J. G., … Advincula, R. (2017). Chitosan cross-linked graphene oxide nanocomposite films with antimicrobial activity for application in food industry. *Macromolecular Symposia*, *374*(1), 1–8. https://doi.org/10.1002/masy.201600114

Gutierrez-Gonzalez, J., Garcia-Cela, E., Magan, N., & Rahatekar, S. S. (2020). Electrospinning alginate/polyethylene oxide and curcumin composite nanofibers. *Materials Letters*, *270*, 127662. https://doi.org/10.1016/j.matlet.2020.127662

Ilhan, E., Pocan, P., Ogawa, M., & Oztop, M. H. (2020). Role of 'D-allulose' in a starch based composite gel matrix. *Carbohydrate Polymers*, *228*-(September 2019), 115373. https://doi.org/10.1016/j.carbpol.2019.115373

Jose, J., & Al-Harthi, M. A. (2017). Citric acid crosslinking of poly (vinyl alcohol)/starch/graphene nanocomposites for superior properties. *Iranian Polymer Journal (English Edition)*, *26*(8), 579–587. https://doi.org/10.1007/s13726-017-0542-0

Kalaycıoğlu, Z., Torlak, E., Akın-Evingür, G., Özen, İ., & Erim, F. B. (2017). Antimicrobial and physical properties of chitosan films incorporated with turmeric extract. *International Journal of Biological Macromolecules*, *101*, 882–888. https://doi.org/10.1016/j.ijbiomac.2017.03.174

Kirtil, E., & Oztop, M. H. (2016). 1H nuclear magnetic resonance relaxometry and magnetic resonance imaging and applications in food science and processing. *Food Engineering Reviews*, *8*(1), 1–22. https://doi.org/10.1007/s12393-015-9118-y

Le Botlan, D., Casseron, F., & Lantier, F. (1998). Polymorphism of sugars studied by time domain NMR. *Analusis*, *26*(5), 198–204. https://doi.org/10.1051/analusis:1998135

Lin, J., Pan, D., Sun, Y., Ou, C., Wang, Y., & Cao, J. (2019). The modification of gelatin films: based on various cross-linking mechanism of glutaraldehyde at acidic and alkaline conditions. *Food Science and Nutrition*, *7*(12), 4140–4146. https://doi.org/10.1002/fsn3.1282

Liu, H., Adhikari, R., Guo, Q., & Adhikari, B. (2013). Preparation and characterization of glycerol plasticized (high-amylose) starch-chitosan films. *Journal of Food Engineering*, *116*(2), 588–597. https://doi.org/10.1016/j.jfoodeng.2012.12.037

Liu, Y., Cai, Y., Jiang, X., Wu, J., & Le, X. (2016). Molecular interactions, characterization and antimicrobial activity of curcumin-chitosan blend films. *Food Hydrocolloids*, *52*, 564–572. https://doi.org/10.1016/j.foodhyd.2015.08.005

Liu, Y., Cai, Z., Sheng, L., Ma, M., Xu, Q., & Jin, Y. (2019). Structure-property of crosslinked chitosan/silica composite films modified by genipin and glutaraldehyde under alkaline conditions. *Carbohydrate Polymers*, *215*(March), 348–357. https://doi.org/10.1016/j.carbpol.2019.04.001

López de Dicastillo, C., Bustos, F., Guarda, A., & Galotto, M. J. (2016). Cross-linked methyl cellulose films with murta fruit extract for antioxidant and antimicrobial active food packaging. *Food Hydrocolloids*, *60*, 335–344. https://doi.org/10.1016/j.foodhyd.2016.03.020

Martucci, J. F., Accareddu, A. E. M., & Ruseckaite, R. A. (2012). Preparation and characterization of plasticized gelatin films cross-linked with low concentrations of Glutaraldehyde. *Journal of Materials Science*, *47*(7), 3282–3292. https://doi.org/10.1007/s10853-011-6167-3

Millar, K. A., Gallagher, E., Burke, R., McCarthy, S., & Barry-Ryan, C. (2019). Proximate composition and anti-nutritional factors of fava-bean (Vicia faba), green-pea and yellow-pea (Pisum sativum) flour. *Journal of Food Composition and Analysis*, *82*(July 2018), 103233. https://doi.org/10.1016/j.jfca.2019.103233

Mohamed, S. A. A., El-Sakhawy, M., & El-Sakhawy, M. A. M. (2020). Polysaccharides, protein and lipid -based natural edible films in food packaging: A review. *Carbohydrate Polymers*, *238*(March), 116178. https://doi.org/10.1016/j.carbpol.2020.116178

Multari, S., Stewart, D., & Russell, W. R. (2015). Potential of fava bean as future protein supply to partially replace meat intake in the human diet. *Comprehensive Reviews in Food Science and Food Safety*, *14*(5), 511–522. https://doi.org/10.1111/1541-4337.12146

Murray, C. A., & Dutcher, J. R. (2006). Effect of changes in relative and temperature on ultrathin chitosan films. *Biomacromolecules*, *7*(12), 3460–3465. https://doi.org/10.1021/bm060416q

Musso, Y. S., Salgado, P. R., & Mauri, A. N. (2017). Smart edible films based on gelatin and curcumin. *Food Hydrocolloids*, *66*, 8–15. https://doi.org/10.1016/j.foodhyd.2016.11.007

Mylläri nen, P., Buleon, A., Lahtinen, R., & Forssell, P. (2002). The crystallinity of amylose and amylopectin films. *Carbohydrate Polymers*, *48*(1), 41–48. https://doi.org/10.1016/S0144-8617(01)00208-9

Narasagoudr, S. S., Hegde, V. G., Chougale, R. B., Masti, S. P., Vootla, S., & Malabadi, R. B. (2020). Physico-chemical and functional properties of rutin induced chitosan/poly (vinyl alcohol) bioactive films for food packaging applications. *Food Hydrocolloids*, *109*(June), 106096. https://doi.org/10.1016/j.foodhyd.2020.106096

Nataraj, D., Sakkara, S., Meghwal, M., & Reddy, N. (2018). Crosslinked chitosan films with controllable properties for commercial applications. *International Journal of Biological Macromolecules*, *120*, 1256–1264. https://doi.org/10.1016/j.ijbiomac.2018.08.187

Ozel, B., Dag, D., Kilercioglu, M., Sumnu, S. G., & Oztop, M. H. (2017). NMR relaxometry as a tool to understand the effect of microwave heating on starch-water interactions and gelatinization behavior. *LWT - Food Science and Technology*, *83*, 10–17. https://doi.org/10.1016/j.lwt.2017.04.077

Ozel, B., Uguz, S. S., Kilercioglu, M., Grunin, L., & Oztop, M. H. (2017). Effect of different polysaccharides on swelling of composite whey protein hydrogels: A low field (LF) NMR relaxometry study. *Journal of Food Process Engineering*, *40*(3), 1–9. https://doi.org/10.1111/jfpe.12465

Pagno, C. H., Klug, T. V., Costa, T. M. H., De Oliveira Rios, A., & Flôres, S. H. (2016). Physical and antimicrobial properties of quinoa flour-based films incorporated with essential oil. *Journal of Applied Polymer Science*, *133*(16), 1–9. https://doi.org/10.1002/app.43311

Pavoni, J. M. F., dos Santos, N. Z., May, I. C., Pollo, L. D., & Tessaro, I. C. (2021). Impact of acid type and glutaraldehyde crosslinking in the physicochemical and mechanical properties and biodegradability of chitosan films. *Polymer Bulletin*, *78*(2), 981–1000. https://doi.org/10.1007/s00289-020-03140-4

Picchio, M. L., Linck, Y. G., Monti, G. A., Gugliotta, L. M., Minari, R. J., & Alvarez Igarzabal, C. I. (2018). Casein films crosslinked by tannic acid for food packaging applications. *Food Hydrocolloids*, *84*(April), 424–434. https://doi.org/10.1016/j.foodhyd.2018.06.028

Pitak, N., & Rakshit, S. K. (2011). Physical and antimicrobial properties of banana flour/chitosan biodegradable and self sealing films used for preserving fresh-cut vegetables. *LWT - Food Science and Technology*, *44*(10), 2310–2315. https://doi.org/10.1016/j.lwt.2011.05.024

Pocan, P., Ilhan, E., & Oztop, M. H. (2019). Effect of D-psicose substitution on gelatin based soft candies: A TD-NMR study. *Magnetic Resonance in Chemistry*, *57*, 661–673. https://doi.org/10.1002/mrc.4847

Priyadarsini, K. I., Maity, D. K., Naik, G. H., Kumar, M. S., Unnikrishnan, M. K., Satav, J. G., & Mohan, H. (2003). Role of phenolic O-H and methylene hydrogen on the free radical reactions and antioxidant activity of curcumin. *Free Radical Biology and Medicine*, *35*(5), 475–484. https://doi.org/10.1016/S0891-5849(03)00325-3

Qiao, C., Ma, X., Wang, X., & Liu, L. (2021). Structure and properties of chitosan films: Effect of the type of solvent acid. *Lwt*, *135*(August 2020), 109984. https://doi.org/10.1016/j.lwt.2020.109984

Ren, L., Yan, X., Zhou, J., Tong, J., & Su, X. (2017). Influence of chitosan concentration on mechanical and barrier properties of corn starch/chitosan films. *International Journal of Biological Macromolecules*, *105*, 1636–1643. https://doi.org/10.1016/j.ijbiomac.2017.02.008

Ritota, M., Gianferri, R., Bucci, R., & Brosio, E. (2008). Proton NMR relaxation study of swelling and gelatinisation process in rice starch-water samples. *Food Chemistry*, *110*(1), 14–22. https://doi.org/10.1016/j.foodchem.2008.01.048

Roy, S., & Rhim, J. W. (2020). Preparation of carbohydrate-based functional composite films incorporated with curcumin. *Food Hydrocolloids*, *98*(July 2019), 105302. https://doi.org/10.1016/j.foodhyd.2019.105302

Roy, S., Zhai, L., Kim, C. H., Pham, H. D., Alrobei, H., & Kim, J. (2021). Tannic-acid-cross-linked and TiO_2-nanoparticle-reinforced chitosan-based nanocomposite film. *Polymers*, *13*, 2–18.

Sauraj, R. P., Kumar, B., & Negi, Y. S. (2018). Chitosan film incorporated with citric acid and glycerol as an active packaging material for extension of green chilli shelf life. *Carbohydrate Polymers*, *195*(December 2017), 329–338. https://doi.org/10.1016/j.carbpol.2018.04.089

Sebti, I., Delves-Broughton, J., & Coma, V. (2003). Physicochemical properties and bioactivity of nisin-containing cross-linked hydroxypropylmethylcellulose films. *Journal of Agricultural and Food Chemistry*, *51*(22), 6468–6474. https://doi.org/10.1021/jf0302613

Seligra, P. G., Medina Jaramillo, C., Famá, L., & Goyanes, S. (2016). Biodegradable and non-retrogradable eco-films based on starch-glycerol with citric acid as crosslinking agent. *Carbohydrate Polymers*, *138*, 66–74. https://doi.org/10.1016/j.carbpol.2015.11.041

Shafie, M. H., Yusof, R., & Gan, C. Y. (2019). Synthesis of citric acid monohydrate-choline chloride based deep eutectic solvents (DES) and characterization of their physicochemical properties. *Journal of Molecular Liquids*, *288*, 111081. https://doi.org/10.1016/j.molliq.2019.111081

Sharma, L., Sharma, H. K., & Saini, C. S. (2018). Edible films developed from carboxylic acid cross-linked sesame protein isolate: Barrier, mechanical, thermal, crystalline and morphological properties. *Journal of Food Science and Technology*, *55*(2), 532–539. https://doi.org/10.1007/s13197-017-2962-4

Silva, S. S., Goodfellow, B. J., Benesch, J., Rocha, J., Mano, J. F., & Reis, R. L. (2007). Morphology and miscibility of chitosan/soy protein blended membranes. *Carbohydrate Polymers*, *70*(1), 25–31. https://doi.org/10.1016/j.carbpol.2007.02.023

Sudhakar, Y. N., Sowmya, & Bhat, D. K. (2012). Miscibility studies of chitosan and starch blends in buffer solution. *Journal of Macromolecular Science, Part A: Pure and Applied Chemistry*, *49*(12), 1099–1105. https://doi.org/10.1080/10601325.2012.728492

Sun, S., Liu, P., Ji, N., Hou, H., & Dong, H. (2018). Effects of various crosslinking agents on the physicochemical properties of starch/PHA composite films produced by extrusion blowing. *Food Hydrocolloids*, *77*, 964–975. https://doi.org/10.1016/j.foodhyd.2017.11.046

Uygun, E., Yildiz, E., Sumnu, G., & Sahin, S. (2020). Microwave pretreatment for the improvement of physicochemical properties of carob flour and rice starch-based electrospun nanofilms. *Food and Bioprocess Technology.*, *13*, 838–850. https://doi.org/10.1007/s11947-020-02440-x

Valizadeh, S., Naseri, M., Babaei, S., Hosseini, S. M. H., & Imani, A. (2019). Development of bioactive composite films from chitosan and carboxymethyl cellulose using glutaraldehyde, cinnamon essential oil and oleic acid. *International Journal of Biological Macromolecules*, *134*, 604–612. https://doi.org/10.1016/j.ijbiomac.2019.05.071

Vargas, C. G., Costa, T. M. H., Rios, A. O., & Flôres, S. H. (2017). Comparative study on the properties of films based on red rice (Oryza glaberrima) flour and starch. *Food Hydrocolloids*, *65*, 96–106. https://doi.org/10.1016/j.foodhyd.2016.11.006

Wu, H., Lei, Y., Lu, J., Zhu, R., Xiao, D., Jiao, C., Xia, R., Zhang, Z., Shen, G., Liu, Y., Li, S., & Li, M. (2019). Effect of citric acid induced crosslinking on the structure and properties of potato starch/chitosan composite films. *Food Hydrocolloids*, *97*(March), 105208. https://doi.org/10.1016/j.foodhyd.2019.105208

Xiao, Q. (2018). Drying process of sodium alginate edible films forming solutions studied by LF NMR. *Food Chemistry*, *250*(December 2017), 83–88. https://doi.org/10.1016/j.foodchem.2018.01.043

Yang, Z., Peng, H., Wang, W., & Liu, T. (2010). Crystallization behavior of poly(ε-caprolactone)/layered double hydroxide nanocomposites. *Journal of Applied Polymer Science*, *116*(5), 2658–2667. https://doi.org/10.1002/app

Yeamsuksawat, T., & Liang, J. (2019). Characterization and release kinetic of crosslinked chitosan film incorporated with α-tocopherol. *Food Packaging and Shelf Life*, *22*(August), 100415. https://doi.org/10.1016/j.fpsl.2019.100415

Yildiz, E., Bayram, I., Sumnu, G., Sahin, S., & Ibis, O. I. (2021). Development of pea flour based active films produced through different homogenization methods and their effects on lipid oxidation. *Food Hydrocolloids*, *111*(August 2020), 106238. https://doi.org/10.1016/j.foodhyd.2020.106238

Yildiz, E., Sumnu, G., & Kahyaoglu, L. N. (2021). Monitoring freshness of chicken breast by using natural halochromic curcumin loaded chitosan/PEO nanofibers as an intelligent package. *International Journal of Biological Macromolecules*, *170*, 437–446. https://doi.org/10.1016/j.ijbiomac.2020.12.160

Yoon, S. D., Chough, S. H., & Park, H. R. (2006). Properties of starch-based blend films using citric acid as additive. *II. Journal of Applied Polymer Science*, *100*(3), 2554–2560. https://doi.org/10.1002/app.23783

Zhao, Y., Teixeira, J. S., Gänzle, M. M., & Saldaña, M. D. A. (2018). Development of antimicrobial films based on cassava starch, chitosan and gallic acid using subcritical water technology. *Journal of Supercritical Fluids*, *137*(December 2017), 101–110. https://doi.org/10.1016/j.supflu.2018.03.010

Zhong, Y., Song, X., & Li, Y. (2011). Antimicrobial, physical and mechanical properties of kudzu starch-chitosan composite films as a function of acid solvent types. *Carbohydrate Polymers*, *84*(1), 335–342. https://doi.org/10.1016/j.carbpol.2010.11.041

Zhou, J., Zhang, J., Ma, Y., & Tong, J. (2008). Surface photo-crosslinking of corn starch sheets. *Carbohydrate Polymers*, *74*(3), 405–410. https://doi.org/10.1016/j.carbpol.2008.03.006

SUPPORTING INFORMATION

Additional supporting information may be found in the online version of the article at the publisher's website.

How to cite this article: Yildiz, E., Ilhan, E., Kahyaoglu, L. N., Sumnu, G., & Oztop, M. H. (2022). The effects of crosslinking agents on faba bean flour–chitosan-curcumin films and their characterization. *Legume Science*, *4*(1), e121. https://doi.org/10.1002/leg3.121